2025 International Conference on Computing, Networking and Communications (ICNC) | 979-8-3315-2096-0/25/$31.00 ©2025 IEEE | DOI: 10.1109/ICNC64010.2025.10993887

A Low-Complexity Post-Distortion Linearization for Satellite and mmWave Communication Systems

Kai Ying*, Linshan Zhao†‡, Yingkai Cao*, Lun Kun§, Danni Li§ and Kai Kang†

*Shanghai Jiao Tong University, Shanghai, China
†Shanghai Advanced Research Institute, Chinese Academy of Sciences, Shanghai, China
‡University of Chinese Academy of Sciences, Beijing, China
§State Key Laboratory of Wireless Mobile Communications, China Academy of Telecommunications Technology, Beijing, China
Email: {yingkai0301, cyk923}@sjtu.edu.cn; {zhaols, kangk}@sari.ac.cn; {kunlun, lidanni}@morningcore.com

***Abstract*—In next-generation wireless communication systems, power amplifier (PA) nonlinearity remains a significant challenge, particularly in high-dynamic and wideband applications such as satellite and millimeter-wave (mmWave) communications. While digital predistortion is a common solution to mitigate PA distortions, its high-complexity and the need of real-time feedback loop create substantial obstacles for modern green communication. In this paper, we propose a low-complexity adaptive digital post-distortion (DPoD) linearization scheme based on orthogonal basis functions. The DPoD approach compensates for PA nonlinearities at the receiver, which can reduce transmitter side complexity while maintaining system performance. The proposed linearization scheme has been validated on real satellite PA and mmWave PA test platforms. Experimental results demonstrate the effectiveness of proposed post-distortion scheme.**

***Index Terms*—Low-complexity, millimeter-wave, power amplifier, post-distortion, satellite communication.**

I. Introduction

The rapid advancement of modern wireless communication systems, including satellite and high-frequency millimeter-wave (mmWave) network, has greatly increased the demand for higher data rates and efficient spectrum utilization [1], [2]. Power amplifiers (PAs), as key nonlinear components in communication systems, introduce significant signal distortions, especially when operated near saturation [3]. The high dynamics in satellite communications and the wide bandwidth requirements in mmWave systems exacerbate these nonlinearities, making distortion even more severe.

Digital predistortion (DPD) has been extensively studied and implemented at the transmitter. It applies an inverse model of the PA's nonlinear characteristics in digital-domain, effectively linearizing the PA output. Many studies have demonstrated the effectiveness of DPD in wireless communication systems [4], [5]. The authors of [6] and [7] provided a detailed analysis of memory polynomial-based DPD techniques in multiple-input multiple-output (MIMO) systems. Besides, the author of [8] and [9] extended these DPD techniques to address the challenges of wide bandwidths and higher frequencies in mmWave communication systems. Additionally, recent work explored machine learning-based DPD further to enhance performance in real-time scenarios [10], [11].

However, DPD introduces significant complexity to the transmitter, requiring real-time feedback loops and high-speed digital processing, which poses challenges for high-performance modern communication systems [12], [13]. In addition, the recently wireless communication standards further relax the limits on out-of-band emission. Compared to strict adjacent channel leakage ratio (ACLR) of LTE systems, which typically enforce values around -45 dBc, the out-of-band ACLR requirement for mmWave high-frequency band is reduced to less than -28 dBc [14]. Given the complexity associated with DPD and the relaxed out-of-band emission limits, there is a growing interest in digital post-distortion (DPoD) techniques. Unlike DPD approach, DPoD operates at the receiver, which can simplify transmitter design while effectively mitigating nonlinearities.

Recent studies have explored various DPoD strategies, investigating their effectiveness in mitigating nonlinearities and enhancing overall system performance. The authors of [15] demonstrated that DPoD scheme could effectively enhance the linearity of PAs in satellite communication systems without the need for complex transmitter configurations. Similarly, the authors of [16] and [17] explored the application of DPoD for mmWave communication systems. However, current research on satellite and mmWave communications mainly relies on simulated data rather than data from real satellite or mmWave PAs. This underscores the critical need for experimental results to provide more convincing and informative insights.

In this paper, we construct physical testing platforms for satellite and mmWave PAs to facilitate demonstration and analysis. The nonlinearity characteristics of high-dynamic satellite PA and wideband mmWave PA are systematically investigated. Furthermore, based on orthogonal basis functions, we propose a low-complexity adaptive DPoD scheme designed for nonlinear satellite and wideband mmWave communication systems. Experimental results demonstrate the effectiveness of the proposed post-distortion scheme.

This paper is organized as follows. Section II introduces the system model. A low complexity adaptive DPoD scheme is proposed in Section III. Experimental results are summarized in Section IV and Section V concludes this paper.

II. System Model and Conventional Adaptive Algorithms

In this paper, we focus on compensating for the nonlinearity of PA. The effects of the wireless channel are assumed to have already been addressed by a channel equalization block prior to the application of DPoD at the receiver side. This assumption allows us to isolate the impact of PA nonlinearity on signal quality and focus on the effectiveness of the proposed DPoD technique.

Considering a general DPoP linearization scheme as shown in Fig. 1. In this figure, up-conversion and down-conversion are omitted to represent equivalently a baseband system. The memory polynomial (MP) model is widely used for the modeling of PA's nonlinearity as well as DPoD function as its simplify and robustness, which is given by [3]

$$\hat{x}(n) = \sum_{m=0}^{M} \sum_{k=1}^{K} \alpha_{2k-1,m} \phi_{2k-1}(n-m), \tag{1}$$

where

$$\phi_{2k-1}(n-m) = y(n-m)|y(n-m)|^{2(k-1)}, \tag{2}$$

and $\alpha_{2k-1,m}$ denote the model coefficients, M and K denote the memory depth and nonlinear order of the model, respectively, $y(n)$ and $\hat{x}(n)$ denote the input and output of the DPoD function, respectively, n denotes the time index of samples. Generally, the model coefficients can be identified by minimizing the error signal $e(n) = x(n) - \hat{x}(n)$, which is given by

$$\min \quad \sum_{n=1}^{N} |e(n)|^2 = \sum_{n=1}^{N} |x(n) - \boldsymbol{\phi}(n)\boldsymbol{\alpha}|^2, \tag{3}$$

where

$$\begin{aligned} \boldsymbol{\phi}(n) &= [\phi_1(n), \ldots, \phi_{2K-1}(n), \ldots, \phi_{2K-1}(n-M)], \\ \boldsymbol{\alpha} &= [\alpha_{1,0}, \ldots, \alpha_{2K-1,0}, \ldots, \alpha_{2K-1,M}]^T. \end{aligned} \tag{4}$$

Traditional adaptive estimation algorithms such as least squares (LS), least mean squares (LMS), and recursive least squares (RLS) are widely used to identify equation (3) [4]. LS algorithm operates on block-sample processing, making it unsuitable for real-time applications. LMS, while computationally simple and feasible for real-time use, suffers from slow convergence, particularly in dynamic environments. RLS provides faster convergence and better performance, making it the most commonly employed algorithm for real-time post-distortion linearization processing. The update equation of RLS solution of (3) is given by [4]

$$\boldsymbol{R}(n) = \left(\boldsymbol{I} - \frac{\boldsymbol{R}(n-1)\boldsymbol{\phi}^H(n)\boldsymbol{\phi}(n)}{\lambda + \boldsymbol{\phi}(n)\boldsymbol{R}(n-1)\boldsymbol{\phi}^H(n)} \right) \boldsymbol{R}(n-1), \tag{5}$$

$$\begin{aligned} \boldsymbol{\alpha}(n) =& \boldsymbol{\alpha}(n-1) \\ &+ \frac{\boldsymbol{R}(n-1)\boldsymbol{\phi}^H(n)}{\lambda + \boldsymbol{\phi}(n)\boldsymbol{R}(n-1)\boldsymbol{\phi}^H(n)} \Big(x(n) - \boldsymbol{\phi}(n)\boldsymbol{\alpha}(n-1) \Big), \end{aligned} \tag{6}$$

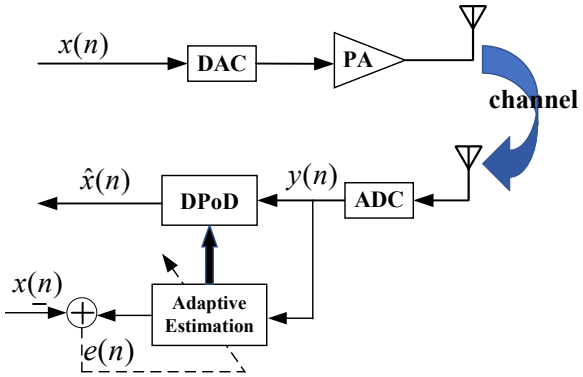

Fig. 1: System diagram of a general adaptive digital post-distortion scheme.

where λ denotes the forgetting factor, closing to 1, $\boldsymbol{R}(n)$ denotes the inversion of $\boldsymbol{\phi}^H\boldsymbol{\phi}$, and $\boldsymbol{R}(0) = \delta^{-1}\boldsymbol{I}$, where δ is an arbitrary small constant, and $\boldsymbol{\alpha}(0)$ is generally defined as $\boldsymbol{\alpha}(0) = [1, 0, \ldots, 0]^T$.

Given the conventional RLS update equation, the computational complexity remains relatively high due to the matrix inversion required at each iteration. This makes it resource-intensive in terms of both processing power and memory, which can be a significant limitation, particularly for real-time systems. In the next section, we will introduce a low-complexity adaptive algorithm.

III. Low-complexity DPoD Linearization Scheme

A. Proposed Adaptive Algorithm

In this paper, we propose a low-complexity RLS adaptive algorithm based on orthogonal basis functions. By utilizing orthogonal polynomials, the conventional matrix inversion required in the RLS algorithm can be avoided. This significantly reduces the computational complexity, making the algorithm more suitable for real-time applications while still maintaining high performance in nonlinear compensation.

Firstly, the orthogonal basis functions for the modeling can be defined as [5]

$$\hat{z}(n) = \sum_{m=0}^{M} \sum_{k=1}^{K} \beta_{2k-1,m} \psi_{2k-1}(n-m), \tag{7}$$

where

$$\psi_{2k-1}(n-m) = \sum_{q=0}^{k} (-1)^{k-q} \frac{\sqrt{k+1}}{(q+1)!} C_k^q \phi_{2k-1}(n-m), \tag{8}$$

and $\beta_{2k-1,m}$ denotes the orthogonal polynomial model coefficients. According to the definition of orthogonal basis functions, we have

$$E\left[\psi_{2k-1}^*(n)\psi_{2p-1}(n)\right] = \begin{cases} 0, & \forall k \neq p, \\ 1, & \forall k = p. \end{cases} \tag{9}$$

We apply the orthogonal basis functions into the update equation of RLS algorithm, $\boldsymbol{R}(n)$ can be rewritten as

$$\boldsymbol{R}(n) = \left(\begin{bmatrix} \boldsymbol{\psi}(1) \\ \boldsymbol{\psi}(2) \\ \vdots \\ \boldsymbol{\psi}(n) \end{bmatrix}^H \begin{bmatrix} \boldsymbol{\psi}(1) \\ \boldsymbol{\psi}(2) \\ \vdots \\ \boldsymbol{\psi}(n) \end{bmatrix} \right)^{-1} \approx \frac{1}{n}\boldsymbol{I}, \quad (10)$$

where $\boldsymbol{\psi}(n) = [\psi_1(n), \ldots, \psi_{2K-1}(n), \ldots, \psi_{2K-1}(n-M)]$. According to the derivation of equation (10), we can further have

$$\frac{\boldsymbol{R}(n-1)\boldsymbol{\psi}^H(n)}{\lambda + \boldsymbol{\psi}(n)\boldsymbol{R}(n-1)\boldsymbol{\psi}^H(n)} \approx \frac{1}{n}\boldsymbol{\psi}^H(n). \quad (11)$$

By incorporating the orthogonal polynomial model and combining equations (10) and (11), the update equation of the RLS algorithm in (6) can be reformulated as

$$\boldsymbol{\alpha}(n) \approx \boldsymbol{\alpha}(n-1) + \frac{1}{n}\Big(x(n) - \boldsymbol{\psi}(n)\boldsymbol{\alpha}(n-1)\Big)\boldsymbol{\psi}^H(n). \quad (12)$$

From (12), we observe that by incorporating orthogonal polynomials into the RLS algorithm, the need for matrix inversion can be bypassed. This modification significantly reduces the computational complexity, allowing for more efficient processing without compromising performance. By eliminating this computational burden, our approach becomes more suitable for real-time applications, enhancing the overall effectiveness of the DPoD processing. Our algorithm performance will be validated in the experiment section.

B. Computational Complexity Analysis

In this subsection, we evaluate the computational complexity of the DPoD estimation algorithm by measuring the number of complex multiplications per iteration. Furthermore, the computational complexity can also be quantified using floating-point operations (FLOPs), which maintains consistency with the complex multiplication metric. Denote $C = (M+1)K$ as the number of DPoD model coefficients. The computational complexity of various adaptive algorithms is summarized in Table I.

TABLE I: Complexity comparisons of different algorithms

Algorithms	Complexity per iteration
LMS	$O(C)$
RLS	$O(C^2)$
Proposed	$O(C)$

From Table I, we observe that applying orthogonal polynomials to the RLS solution, the computational complexity of the proposed adaptive algorithm is on the order of $O(C)$ per iteration, which is comparable to that of the LMS algorithm. At the same time, the proposed algorithm also maintains the fast convergence characteristics of the RLS. This combination of reduced overall complexity and enhanced convergence speed makes our approach particularly effective for real-time applications in DPoD linearization scheme, ensuring efficient processing without sacrificing performance.

IV. Experimental Results

In this section, we construct real physical wideband mmWave PA and high-dynamic satellite PA test platforms to demonstrate the performance of the proposed algorithm, as illustrated in Fig. 2.

The input signals are 64-quadrature amplitude modulation (64-QAM) orthogonal frequency division multiplexing (OFDM) signals. For the mmWave PA test platform, shown in Fig. 2(a), an arbitrary waveform generator (AWG) is used to load the baseband signal onto a 135-GHz carrier through a mixer and frequency , amplified by mmWave PA, then down-converted and captured by an oscilloscope. Similarly, for the satellite PA test, shown in Fig. 2(b), the input baseband signal is up-converted to the Ka frequency band at 29.5 GHz, amplified by the satellite PA, and subsequently down-converted to obtain the received baseband signal. Error vector magnitude (EVM) and ACLR are used to evaluate the linearization performance of the proposed algorithm.

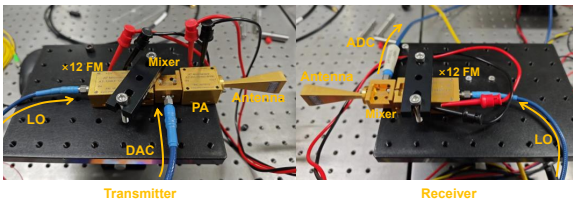

(a) mmWave PA test bench

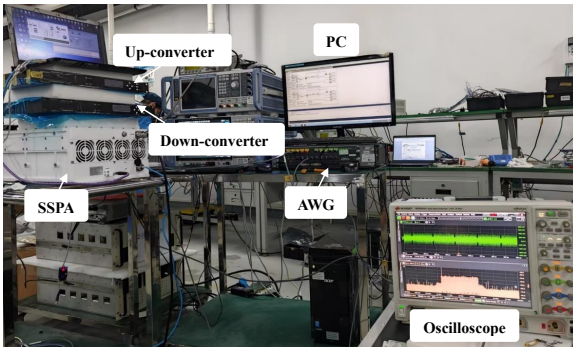

(b) satellite PA test bench

Fig. 2: Experiment platforms for wideband mmWave PA and satellite PA.

We first validate the algorithm performance on wideband mmWave PA test platform. The input signal bandwidth is configured to 1 GHz and 2 GHz, respectively. For comparison, the proposed DPoD scheme and the conventional LMS algorithm are implemented with identical coefficient configurations to compensate for the PA's nonlinearity. For the DPoD scheme, the coefficients are set to $M = 8$, $K = 4$ for the 1 GHz bandwidth scenario and $M = 10$, $K = 4$ for the 2 GHz bandwidth scenario. Fig. 3 depicts the normalized power spectrum densities (PSDs) of the received signal with different input bandwidths. The corresponding constellation diagrams are shown in Fig. 4. The EVM and ACLR values are summarized in Table II.

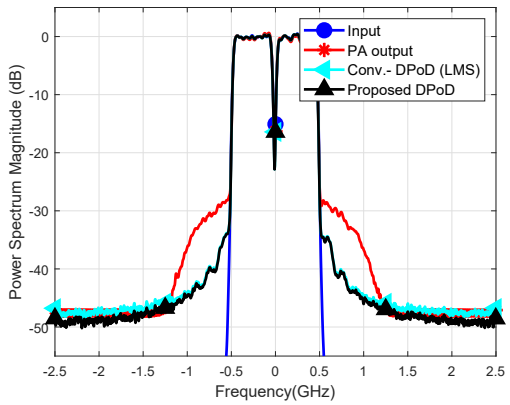

(a) 1 GHz bandwidth

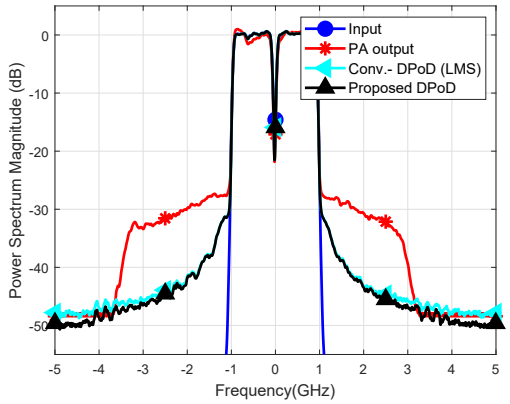

(b) 2 GHz bandwidth

Fig. 3: The normalized PSDs of received signal with different input bandwidths on mmWave PA test platform.

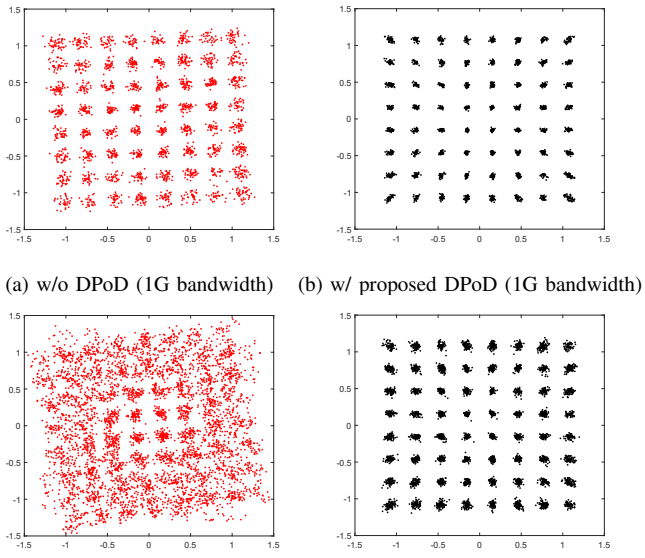

(a) w/o DPoD (1G bandwidth) (b) w/ proposed DPoD (1G bandwidth)

(c) w/o DPoD (2G bandwidth) (d) w/ proposed DPoD (2G bandwidth)

Fig. 4: Constellation diagrams of 64-QAM OFDM signal with different input bandwidths on mmWave PA test.

TABLE II: ACLR and EVM on mmWave PA test scenario

1GHz bandwidth input			
	w/o DPoD	w/ conv.-DPoD (LMS)	proposed DPoD
ACLR (dBc)	-33.01	-41.43	-41.92
EVM (dB)	-22.26	-31.84	-32.28
2GHz bandwidth input			
	w/o DPoD	w/ conv.-DPoD (LMS)	proposed DPoD
ACLR (dBc)	-29.33	-39.29	-39.89
EVM (%)	-14.28	-29.01	-29.61

From experimental results for the mmWave PA, we observe that the proposed DPoD achieves satisfactory linearization performance. The performance of the conventional LMS-based DPoD algorithm is similar to that of the proposed algorithm. For the 1 GHz input, the proposed algorithm demonstrates about 8 dB improvement in out-of-band ACLR performance and 10 dB improvement in in-band EVM performance. For the 2 GHz input, the proposed DPoD algorithm provides over 10 dB enhancement in out-of-band ACLR performance and 15 dB improvement in in-band EVM performance, highlighting a more pronounced performance advantage as the bandwidth increases. These results validate the effectiveness of the proposed approach in high-frequency applications.

Next, we validate the performance on satellite PA test platform. The bandwidth of the input signal is configured to 100 MHz and the DPoD coefficients are set to $M = 10$ and $K = 5$. Fig. 5 and Fig. 6 show the PSDs of the received signals and constellation diagrams, respectively. The corresponding ACLR and EVM are listed in Table III.

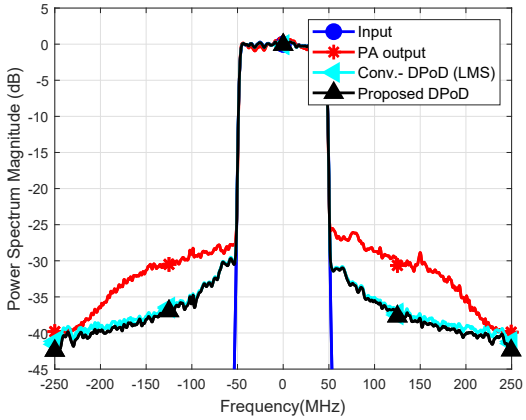

Fig. 5: The normalized PSDs of the received signal on satellite PA test platform.

TABLE III: ACLR and EVM on satellite PA test scenario

	w/o DPoD	w/ conv.-DPoD (LMS)	proposed DPoD
ACLR (dBc)	-28.01	-35.12	-35.56
EVM (dB)	-20.91	-28.54	-29.12

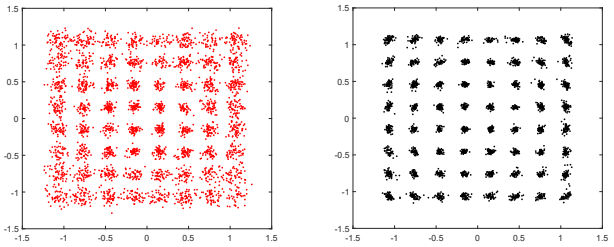

(a) w/o DPoD (b) w/ proposed DPoD

Fig. 6: Constellation diagrams of 100MHz 64-QAM OFDM signal on satellite PA test.

From the experimental results for the satellite PA, we observe that the proposed DPoD scheme achieves satisfactory linearization performance. Specifically, the proposed algorithm provides approximately 7 dB of out-of-band spectral suppression and 9 dB improvement in in-band EVM. These experimental results demonstrate the robustness of the proposed DPoD scheme on the satellite PA test platform, confirming its ability to effectively mitigate PA nonlinearity while maintaining signal integrity.

In terms of computational complexity, we compare the convergence speed of the proposed DPoD algorithm with that of the conventional LMS-based DPoD algorithm, as illustrated in Fig. 7.

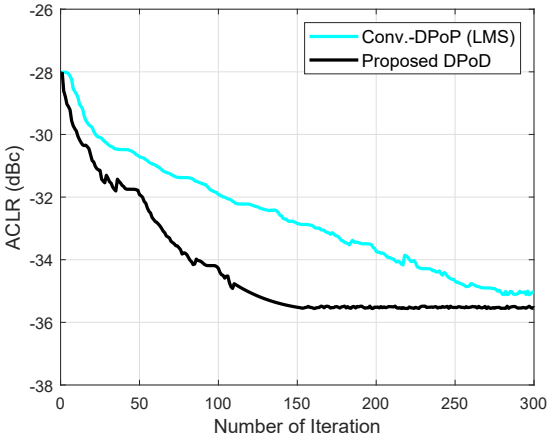

Fig. 7: Comparisons of convergence speed.

From Fig. 7, we observe that the proposed DPoD algorithm demonstrates significantly faster convergence compared to the conventional based-LMS DPoD algorithm, which results in a notable reduction in computational complexity. This complexity reduction, discussed in Section III-B, makes the adaptive algorithm more suitable for real-time applications while maintaining satisfactory linearization performance.

V. Conclusion

In this paper, we propose a low-complexity adaptive DPoD linearization scheme based on orthogonal basis functions for high-dynamic satellite and wideband millimeter-wave communication systems. Our approach effectively bypasses the matrix inversion typically required in conventional RLS algorithms, significantly reducing computational complexity while maintaining fast convergence. Experimental results demonstrated that the proposed DPoD algorithm can achieve satisfactory performance in both out-of-band ACLR and in-band EVM. The validation on real physical test platforms reinforces the effectiveness and practicality of the proposed algorithm.

References

[1] W. Yi, W. Zhiqing and F. Zhiyong, “Beam training and tracking in mmWave communication: A survey," China Communications, vol. 21, no. 6, pp. 1-22, June 2024.

[2] J. Heo, S. Sung, H. Lee, I. Hwang and D. Hong, “MIMO Satellite Communication Systems: A Survey From the PHY Layer Perspective," IEEE Communications Surveys & Tutorials, vol. 25, no. 3, pp. 1543-1570, thirdquarter 2023.

[3] L. Ding, G. T. Zhou, D. R. Morgan, Z. Ma, J. S. Kenney, J. Kim, and C. R. Giardina, “A robust digital baseband predistorter constructed using memory polynomials," IEEE Transactions on Communications, vol. 52, no. 1, pp. 159-165, 2004.

[4] J. Chani-Cahuana, P. N. Landin, C. Fager, and T. Eriksson, “Iterative learning control for RF power amplifier linearization," IEEE Transactions on Microwave Theory and Techniques, vol. 64, no. 9, pp. 2778-2789, 2016.

[5] R. Raich, H. Qian, and G. T. Zhou, “Orthogonal polynomials for power amplifier modeling and predistorter design," IEEE Transactions on Vehicular Technology, vol. 53, no. 5, pp. 1468-1479, 2004.

[6] Shipra, G. C. Tripathi, and M. Rawat, “Power amplifier linearization in the presence of crosstalk and measurement noise in MIMO system," IEEE Transactions on Circuits and Systems II: Express Briefs, vol. 69, no. 10, pp. 3988-3992, 2022.

[7] M. B. Salman, A. B. Ucuncu and G. M. Guvensen, “Reduced Complexity Correlation-Based Multi-Stream DPD for Hybrid Massive MIMO," IEEE Communications Letters, vol. 28, no. 3, pp. 677-681, 2024.

[8] A. Ben Ayed, Y. Cao, P. Mitran and S. Boumaiza, “Digital Predistortion of Millimeter-Wave Arrays Using Near-Field Based Transmitter Observation Receivers," IEEE Transactions on Microwave Theory and Techniques, vol. 70, no. 7, pp. 3713-3723, 2022.

[9] H. Yin et al., “Data-Clustering-Assisted Digital Predistortion for 5G Millimeter-Wave Beamforming Transmitters With Multiple Dynamic Configurations," IEEE Transactions on Microwave Theory and Techniques, vol. 69, no. 3, pp. 1805-1816, 2021.

[10] Muskatirovic-Zekic T, Neskovic N, Budimir D., “Efficient neural network DPD architecture for hybrid beamforming mMIMO," Electronics, 2023, 12(3): 597.

[11] X. Cheng, R. Zayani, M. Ferecatu and N. Audebert, “Efficient Autoprecoder-based deep learning for massive MU-MIMO Downlink under PA Non-Linearities," 2022 IEEE Wireless Communications and Networking Conference (WCNC), Austin, TX, USA, 2022.

[12] F. Ma, F. Guo, L. Yang, “Low-complexity TDOA and FDOA localization: A compromise between two-step and DPD methods," Digital Signal Processing, vol. 96, 2020.

[13] L. Zhao, H. Qian, W. Feng, M. Li and K. Kang, “A Low-Complexity Digital Predistorter for Large-Scale MIMO Systems With Crosstalk," IEEE Transactions on Vehicular Technology, vol. 72, no. 10, pp. 13203-13213, 2023.

[14] “5G; NR; Base station (BS) radio transmission and reception (Release 15)," 3GPP Technical Specification (TS), vol. 38, no. 104, 2021.

[15] Q. Chen, Z. Wang, G. F. Pedersen and M. Shen, “Joint satellite-transmitter and ground-receiver digital pre-distortion for active phased arrays in LEO satellite communications", Remote Sensor, vol. 14, no. 17, pp. 4319, 2022.

[16] H. Babaroglu, L. Anttila, G. Xu, M. Turunen, M. Allen and M. Valkama, “Cellular Digital Post-Distortion: Signal Processing Methods and RF Measurements," 2023 IEEE Wireless and Microwave Technology Conference (WAMICON), Melbourne, FL, USA, 2023.

[17] J. Pihlajasalo et al., “Deep Learning OFDM Receivers for Improved Power Efficiency and Coverage," IEEE Transactions on Wireless Communications, vol. 22, no. 8, pp. 5518-5535, 2023.